Optics Communications 297 (2013) 141–146

Contents lists available at SciVerse ScienceDirect

Optics Communications

journal homepage: www.elsevier.com/locate/optcom

Switchable tunneling mode for cylindrical photonic quantum well consisting of photonic crystals containing liquid crystal

C.A. Hu [a,*], S.L. Yang [a], T.J. Yang [b]

[a] Department of Electrophysics, National Chiao Tung University, No. 1001, Daxue Rd., East Dist., Hsinchu City 30010, Taiwan, ROC
[b] Department of Electrical Engineering, Chung Hua University, No. 707, Sec. 2, WuFu Rd., Xiangshan Dist., Hsinchu City 30012, Taiwan, ROC

ARTICLE INFO

Article history:
Received 7 September 2012
Received in revised form
6 December 2012
Accepted 9 December 2012
Available online 16 January 2013

Keywords:
Photonic quantum well
Tunneling mode
Transfer matrix method

ABSTRACT

We propose a cylindrical photonic quantum well made of photonic crystals containing liquid crystals, the properties of which are theoretically calculated and investigated by the transfer matrix method in the cylindrical symmetry system. Liquid crystals are introduced into the photonic quantum well structure as tunable defect layers. When the liquid crystals are pseudo–isotropic state and the azimuthal mode order of incident waves are $m=0$, there were two pass-bands around certain wavelength. When the liquid crystals are homeotropic state, the reflectance of pass-band at shorter wavelength decreases from 0.75 to 0.05 in the TM mode, but the reflectance does not change in the TE mode. When mode order $m=1$ and the liquid crystals are pseudo-isotropic state, the reflectance of defect mode stayed the same as $m=0$. However, the result is reversed while the phase of liquid crystals change from pseudo-isotropic to homeotropic state. The reflectance is the same as in the TM mode, but that in the TE mode decreases substantially from 0.75 to 0.05. The application of our structure to switching device is highly potential.

1. Introduction

Photonic crystal (PC) is a composite material with permittivity and permeability in one, two or three dimensions periodic structure [1–3].The studies of PC have attracted a large number of interests for their capability in prohibiting certain frequency-range of electromagnetic (EM) waves from propagating in such structure over the past decade. These frequency regions are called photonic band gaps (PBGs), which is the most prominent characteristic and can lead to many potential applications [4–6].

In the past few years, Bragg reflectors (BRs) have been playing an important role in optical components. ABR is a periodic multilayer structure that has switching layers of a material with a lower refractive index and one with a higher refractive index. It can suppress undesired interfacial Fresnel reflection over a wide range of wavelengths. As the number of periods becomes large, a BR could be analogous to a one dimensional PC [7]. The transfer-matrix method (TMM) is typically used to analyze EM waves propagate through an optical device, especially in 1 DPC. Recently, the TMM was developed to calculate PBGs for cylindrical EM waves that propagate through a structure with cylindrical symmetry [8]. Base on the establishment of the TMM in the cylindrical symmetry system, it has attracted much attention for the studies of EM properties of annular Bragg reflector (ABR). Some related theoretical investigations that cylindrical EM waves propagate in an ABR have been reported recently [9,10], such as reflection properties at an interface with small starting radius and the difference between the E-polarization and H-polarization for a higher azimuthal mode and so on. However, some interesting features of ABR still require further investigation.

On the other hand, for applications, PCs with tunable properties have also attracted a great deal of attention in the recent years [11–14]. Some tunabilities which can control the number of filter modes by inserting a defect layer. For example, Bhuvneshwer and Bhargava used photonic quantum well structures and inserted defect layer to achieve multi-channel filter modes in the photonic band gap region [15]. The number of defect filter mode can be tuned by adjusting the number of defect layers. Hsu et al. introduced the defect band in the PBG with coupled impurities in a quarter-wavelength stack to achieve multichannel transmission filter [16]. The number of defect modes is equal to the number of coupled impurity layers. Zhao. et al. also demonstrated that with the increase of the layer number of PQWs, the resonant transmissivtity of confined modes is reduced gradually and the number of confined modes is increased with the increasing number of defect layers [17]. This kind of tunability is usually used as a filter.

Some tunabilities which will change the position of PBG during operation. This kind of tunable capacity depends on adjustment of the permittivity or permeability of constituent materials by some

* Corresponding author. Tel.: +886 928635096; fax: +88635725230.
E-mail address: markhu24@gmail.com (C.A. Hu).

0030-4018/$ - see front matter Crown Copyright © 2013 Published by Elsevier B.V. All rights reserved.
http://dx.doi.org/10.1016/j.optcom.2012.12.054

external parameters such as temperature, external magnetic fields or electric fields. Due to tunable features, PC can be designed and utilized extensively in optoelectronic devices and microwave communication system. One of the prospective materials for fabricating tunable PC is liquid crystals (LCs) due to their characteristics of optical anisotropy and dielectric anisotropy based on the molecular orientation order. Thermal forces are also employed for the reorientation of LC molecules in PC structures to possess the tuning property. The variation of the refractive index due to electro–optical effect can reach up to $\Delta n=0.2$ which is much larger than the variation cause by thermal forces. However, most works paid attention on thermal tuning effect rather than electrical tuning effect.

In this paper, we focus on the electro–optical effect of LCs and introduce LCs into a cylindrical photonic crystal as defect layers. First, we take advantage of the concept of photonic quantum well (PQW) structure [15–17] to broaden the PBGs for the azimuthal mode number $m=0$ and $m=1$. By introducing LCs into the structure, a tunable photonic defect mode will be obtained. Owing to the variation of refractive index of LCs via an applied electric field, a tunable defect mode is observed for the azimuthal mode number $m=0$ and $m=1$. However, the feature of defect mode will be reversed for the azimuthal mode number $m=1$. This interesting phenomenon has not been exploited up to the present in our knowledge.

The rest of this paper is organized as follows: in Section 2, the TMM for cylindrical waves in an annular cylindrical structure was illustrated to calculate the reflectance spectrum for different azimuthal mode. In Section 3, the effect of starting radius is discussed. Then, the concept of PQW structure was used to broaden the PBGs. Besides, LCs were then used to create a tunable feature. Finally, the results of calculation were discussed and then summarized.

2. Theory

The TMM for calculating the reflectance spectrum in cylindrical symmetry structures [8] is briefly described. The method is applied to investigate the propagation of cylindrical EM waves in different polarization and for different azimuthal mode through each cylindrical interface. As illustrated in Fig. 1(a), there is an annular cylindrical structure consists of multilayer media. The boundary of inner core is formed the first layer, where the core radius ρ_0 is also called the starting radius. For the next layer, the label ρ_1 is the radius from the center of structure to the interface between layer 1 and layer 2 and so forth. The refractive index of the core, material 1, material 2 and the surrounding materials are represented by n_0, n_1, n_2, n_f.We assume that the cylindrical structure has an infinite length from $z=0$ to $z=\infty$. A linear source is inserted inside the core of starting radius to generate cylindrical EM waves, hence cylindrical EM waves propagate along ρ axis from $\rho=0$ to $\rho=\infty$, which incident on each interface normally. The reflectance at the interface can be obtained by using TMM in cylindrical symmetry system. Fig. 1(b) and (c) are TE and TM directions on top of the cross-section geometry of cylindrical structure. Generally speaking, Maxwell equation can be rewritten in cylindrical coordinate form as following:

$$\rho\frac{\partial}{\partial\rho}\left(\rho\frac{\partial E_z}{\partial\rho}\right)-\rho^2\frac{1}{\mu}\frac{\partial\mu}{\partial\rho}\frac{\partial E_z}{\partial\rho}+\frac{\partial}{\partial\phi}\left(\frac{\partial E_z}{\partial\phi}\right)+\omega^2\mu\varepsilon\rho^2E_z=0 \tag{1}$$

This equation is the governing differential equation in the TE mode. To solve Eq. (1), we used the method of separation of variables and let $E_z=V(\rho)\Phi(\phi)$, where $\Phi(\phi)=\exp(jm\phi)$. The radial part V satisfies

$$\rho\frac{\partial}{\partial\rho}\left(\rho\frac{\partial V}{\partial\rho}\right)+\left(k^2\rho^2-m^2\right)V=0 \tag{2}$$

This is Bessel's equation with the solution

$$V(\rho)=AJ_m(k\rho)+BY_m(k\rho) \tag{3}$$

where A and B are constant, J_m is a Bessel function, Y_m is a Neumann function, $k=\omega\sqrt{\mu\varepsilon}=n\omega/c$ and m is an integer which is referred to as the azimuthal mode number. In the similar way, magnetic field $H_\phi=U(\rho)e^{jm\phi}$ is assumed. We have

$$U(\rho)=\frac{1}{j\omega\mu}\frac{\partial V}{\partial\rho}=\frac{k}{j\omega\mu}\left(AJ'_m(k\rho)+BY'_m(k\rho)\right) \tag{4}$$

Let us rewrite Eq. (4) as

$$U(\rho)=-jp\left(AJ'_m(k\rho)+BY'_m(k\rho)\right) \tag{5}$$

where p is defined as the intrinsic admittance of the medium.

$$\frac{k}{j\omega\mu}=-j\frac{\omega\sqrt{\mu\varepsilon}}{\omega\mu}=-j\sqrt{\frac{\varepsilon}{\mu}}=-jp \tag{6}$$

Combine Eqs. (3) and (5) to establish the relationship of transfer matrix M_1 is expressed as

$$\begin{bmatrix}V(\rho_1)\\U(\rho_1)\end{bmatrix}=M_1\begin{bmatrix}V(\rho_0)\\U(\rho_0)\end{bmatrix}=\begin{bmatrix}m_{11}&m_{12}\\m_{21}&m_{22}\end{bmatrix}\begin{bmatrix}V(\rho_0)\\U(\rho_0)\end{bmatrix} \tag{7}$$

each matrix elements of M_1 is written as

$$\begin{aligned}
m_{11}&=\frac{\pi}{2}k_1\rho_0\left[Y'_m(k_1\rho_0)J_m(k_1\rho_1)-J'_m(k_1\rho_0)Y_m(k_1\rho_1)\right]\\
m_{12}&=j\frac{\pi}{2}\frac{k_1}{p_1}\rho_0\left[J_m(k_1\rho_0)Y_m(k_1\rho_1)-Y_m(k_1\rho_0)J_m(k_1\rho_1)\right]\\
m_{21}&=-j\frac{\pi}{2}k_1p_1\rho_0\left[Y'_m(k_1\rho_0)J'_m(k_1\rho_1)-J'_m(k_1\rho_0)Y'_m(k_1\rho_1)\right]\\
m_{22}&=\frac{\pi}{2}k_1\rho_0\left[J_m(k_1\rho_0)Y'(k_1\rho_1)-Y_m(k_1\rho_0)J'_m(k_1\rho_1)\right]
\end{aligned} \tag{8}$$

where $p_1=\sqrt{\varepsilon_1/\mu_1}$. Similarly, we can obtain the transfer matrix M_i for each layer and the total system matrix M can be found by

$$\begin{bmatrix}V(\rho_f)\\U(\rho_f)\end{bmatrix}=M\begin{bmatrix}V(\rho_0)\\U(\rho_0)\end{bmatrix}=\begin{bmatrix}M_{11}&M_{12}\\M_{21}&M_{22}\end{bmatrix}\begin{bmatrix}V(\rho_0)\\U(\rho_0)\end{bmatrix}=M_i\cdots M_3M_2M_1\begin{bmatrix}V(\rho_0)\\U(\rho_0)\end{bmatrix} \tag{9}$$

According to the matrix elements in Eq. (9), we can define the elements of the inverse matrix of M by M'_{11}, M'_{12}, M'_{21} and M'_{22}. Therefore, we will have the reflection and transmission coefficients as follows for E-polarization:

$$r_d=\frac{\left(M'_{21}+jp_0C^{(2)}_{m0}M'_{11}\right)-jp_fC^{(2)}_{mf}\left(M'_{22}+jp_0C^{(2)}_{m0}M'_{12}\right)}{\left(-jp_0C^{(1)}_{m0}M'_{11}-M'_{21}\right)-jp_fC^{(2)}_{mf}\left(-jp_0C^{(1)}_{m0}M'_{12}-M'_{22}\right)} \tag{10}$$

$$t_d=\frac{4\sqrt{\varepsilon_0/\mu_0}}{\pi K\rho_0H^{(2)}_m(k_0\rho_0)H^{(1)}_m(k_0\rho_0)\left[\left(-jp_0C^{(1)}_{m0}M'_{11}-M'_{21}\right)-jp_fC^{(2)}_{mf}\left(-jp_0C^{(1)}_{m0}M'_{12}-M'_{22}\right)\right]} \tag{11}$$

where $H^{(1)}_m$ and $H^{(2)}_m$ are the Hankel function of the first and second kind, $K=\omega\sqrt{\mu_0\varepsilon_0}$, $p_0=\sqrt{\varepsilon_0/\mu_0}$, $p_f=\sqrt{\varepsilon_f/\mu_f}$and

$$C^{(1,2)}_{ml}=\frac{H^{(1,2)\prime}_m(k_l\rho_l)}{H^{(1,2)}_m(k_l\rho_l)},\quad l=0,f \tag{12}$$

Similarly, we exchanged ε with μ and j with $-j$ in the formulations of reflection and transmission coefficient, the corresponding results for H-polarization can be acquired.

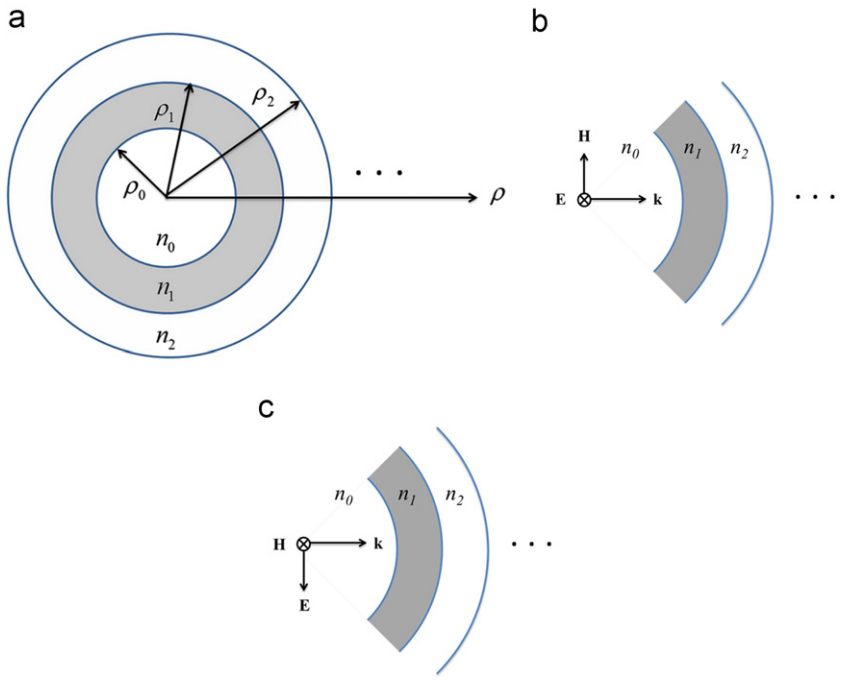

Fig. 1. (a) The representation and cross-section geometry of the cylindrical structure. The schematic represents (b) TE and (c) TM directions on top of the cross-section geometry of the cylindrical structure.

In our works, TM method is different from solving partial differential Eq. (1) to include all set of azimuthal mode terms. We investigate transmission properties of each azimuthal mode in TE (TM) mode propagating outward through multilayers. In our work, there are only two azimuthal modes $m=0$ and $m=1$ to be considered, other higher order modes neglected.

3. Results and discussion

To present the numerical results, we first investigate the reflection properties in a single cylindrical PC (CPC) which is constructed of silicon and air. Unlike in the usual planar interface, the starting radius ρ_0 in Fig. 1 may play an important role in the study of wave properties in a cylindrical system. Fig. 2 depicts the reflectance versus wavelength with starting radius $\rho_0=80$ nm, $\rho_0=400$ nm, and $\rho_0=800$ nm at different azimuthal mode $m=0$ and $m=1$, respectively. Here, $n_0=n_2=1$, $n_1=3.6$ and $ff=0.55$ are chosen. Here ff represents filling factor (or fill fraction), which is defined as a relative percentage of area of silicon composing a unit cell. For E-polarization (Fig. 2(a)), the reflectance is almost unchanged when the starting radius is increased from $\rho_0=80$ nm to $\rho_0=800$ nm at azimuthal mode $m=0$. At $m=1$, the reflectance spectrum shift slightly toward longer wavelength when the starting radius increased. We can also observe that the reflectances of oscillation peaks outside the PBGs are decreased in Fig. 2(c). For H-polarization, the reflectance is decreasing function of ρ_0 at azimuthal mode $m=0$ and $m=1$. The reflectance spectrum at $m=0$ is similar to E-polarization at $m=1$. But, quick drops in reflectance can be observed at wavelength $\lambda=380$ nm to $\lambda=470$ nm when the starting radius increased at $m=1$.When the wavelength longer than $\lambda=620$ nm, the reflectance oscillations of small radius are counter to that of longer starting radius. Conclusively, the reflectance for both polarization modes can be significantly changed as a function of the starting radius when ρ_0 is small at azimuthal mode $m>0$.

To investigate the PBGs for high order azimuthal mode, the concept of a PQW structure in the cylindrical symmetric system is utilized. At first, two kinds of material constitute cylindrical photonic quantum well (CPQW) structure and the photonic band gaps of type 1 and type 2 from $ff=0.10$ to $ff=0.95$ are calculated by the plane wave method (PWM). From band dispersion diagrams, we can set the position of the PBGs in the reflectance spectrum by tuning the filling factor. Two type of CPQW structures are chosen: type 1 $(AB)_p$ is constructed of silicon for A and air for B whose filling factor is $ff=0.55$; type 2 $(AC)_p$ is constructed of silicon for A and LC for C whose filling factor is $ff=0.69$ where p is the number of unit cell, respectively. We choose $ff=0.55$ for type 1 and $ff=0.69$ for type 2 because of their PGBs are adjacent. The diagrams that represent type 1 and type 2 PC structure are shown in Fig. 3(a) and (b). Fig. 4(a) and (b) shows the band diagrams of type 1 and type 2 calculated by PWM where the refractive indices are $n_{Si}=3.6$, $n_{air}=1$ and $n_{LC}=1.56$. As indicated in figures, there are many small PBGs in type 1 and type 2. All of PBGs are marked by shaded areas. If we could connect these PBGs together, we will obtain a broaden PBG between normalized frequency 0.15–0.95.The reflectance spectra of the corresponding band diagrams of type 1 and type 2 in the wavelength range 300 nm–1100 nm when the incident wave is E (dashed line) and H polarized (solid line) are shown in Fig. 5(a) and (b) where the starting radius and the number of unit cell are assume to be $\rho_0=80$ nm and $p=8$. In reflectance spectra, the first PBG of type 1 locates at wavelength $\lambda=325$ nm to $\lambda=375$ nm and the second PBG locates at $\lambda=470$ nm to $\lambda=620$ nm; the first PBG of type 2 locates at $\lambda<320$ nm,the second PBG locates at $\lambda=360$ nm to $\lambda=440$ nm and the third PBG locates at $\lambda=540$ nm to $\lambda=690$ nm. The second PBG of type 2 is between the two PBGs of type 1. Thus, we take advantage of the concept of PQW structure in order to broaden the PBG. We use type 1 as barrier PCs to sandwich type 2 which is treated as a well PC as shown in Fig. 3(c). Fig. 6(a) and (b) shows that the reflectance spectrum of the CPQW $(AB)_4(AC)_4(AB)_4$ in the TE (dashed line) and TM mode (solid line) for azimuthal mode $m=0$ and $m=1$. The CPQW structure which is composed of type 1 with filling factor $ff=0.55$ and type 2 with filling factor $ff=0.69$, respectively. The PBG of the CPQW structure is located at the range from $\lambda=420$ nm to $\lambda=920$ nm. It is demonstrated that the PBG is widened successfully not only for mode order $m=0$, but also for $m=1$. However, the PBG in

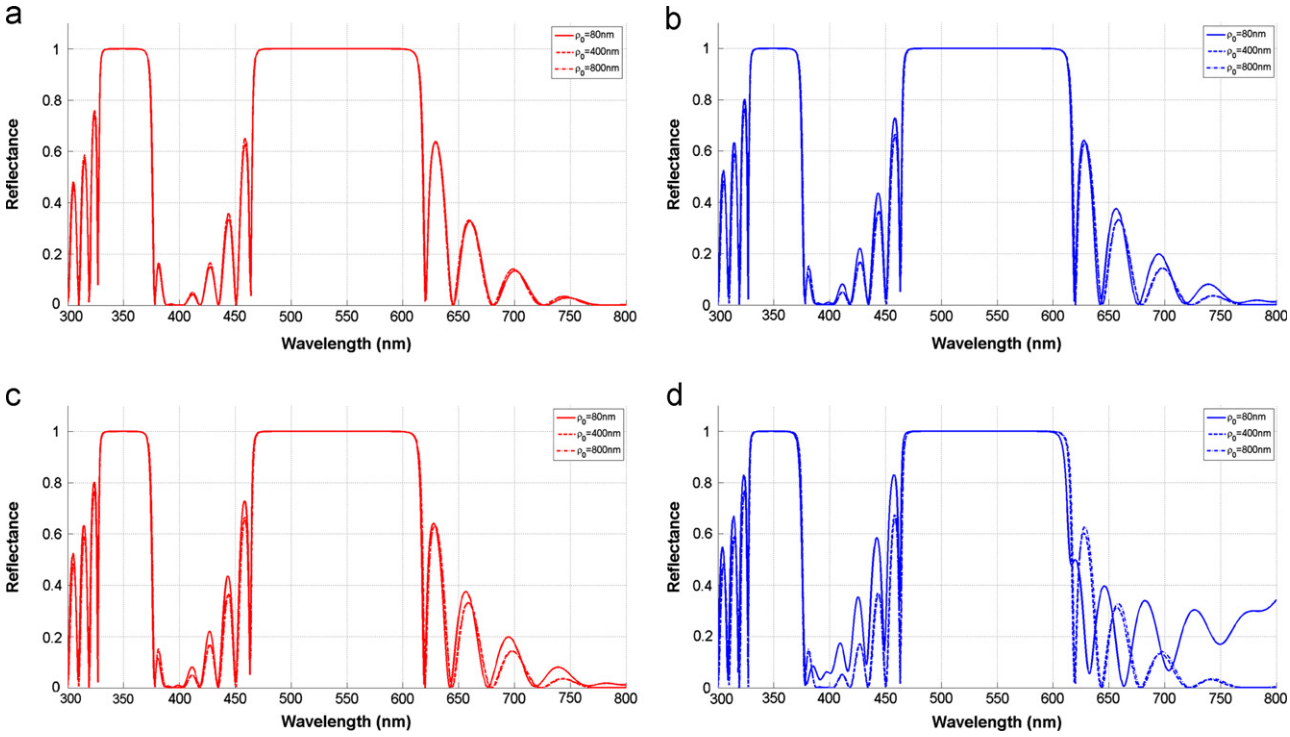

Fig. 2. The schematic represents (a) type 1 PC structure, (b) type 2 PC structure and (c) photonic quantum well structure.

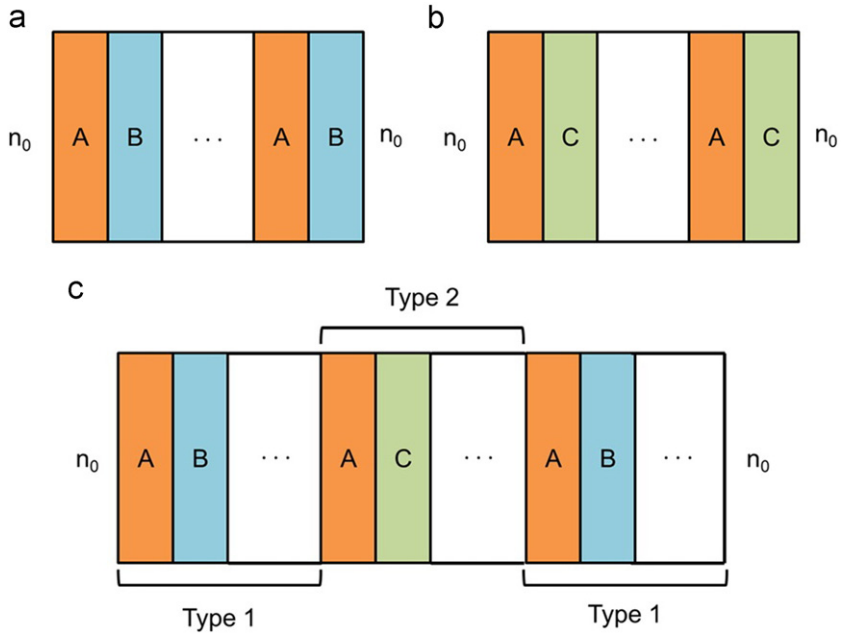

Fig.3. The reflectance versus wavelength with different starting radius for (a) E-polarization and (b) H-polarization at azimuthal mode $m=0$, and for (c) E-polarization and (d) H-polarization at azimuthal mode $m=1$, respectively. (a) Type 1, (b) Type 2 and (c) Photonic quantum well structre.

the TM mode for azimuthal mode $m=1$ was widened larger toward longer wavelength than that in the TE mode as shown in Fig. 6(b). As the starting radius ρ_0 is increased gradually, the phenomenon of the PBG in the TM mode which is wider than that in TE mode will gradually vanish. Therefore, the PBG of CPQW structure for H-polarization wave for azimuthal mode $m=1$ is sensitive to the starting radius but the PBG for E-polarization wave is insensitive. According to the difference of reflectance spectra between TE and TM mode cause by small starting radius effect, we set the starting radius $\rho_0=80$ nm in the following calculations.

Further, we used the property of LCs to create a tunable defect mode. First, we adjusted the filling factor of type 2 from 0.69 to 0.72 in order to match a partial of PBG of type 1 and pass-band of type 2 to create a narrow defect mode. An external electric field $E=2.78\times10^6(V/m)$ is applied to the CPQW structure which is used to control the refractive index of the LCs in the simulation. The electric field which is radially outward from the center of the CPQW structure in all direction, the state of the LCs will transform from pseudo-isotropic to homeotropic when the electric field is turned on. At first, the LC is pseudo-isotropic state and the

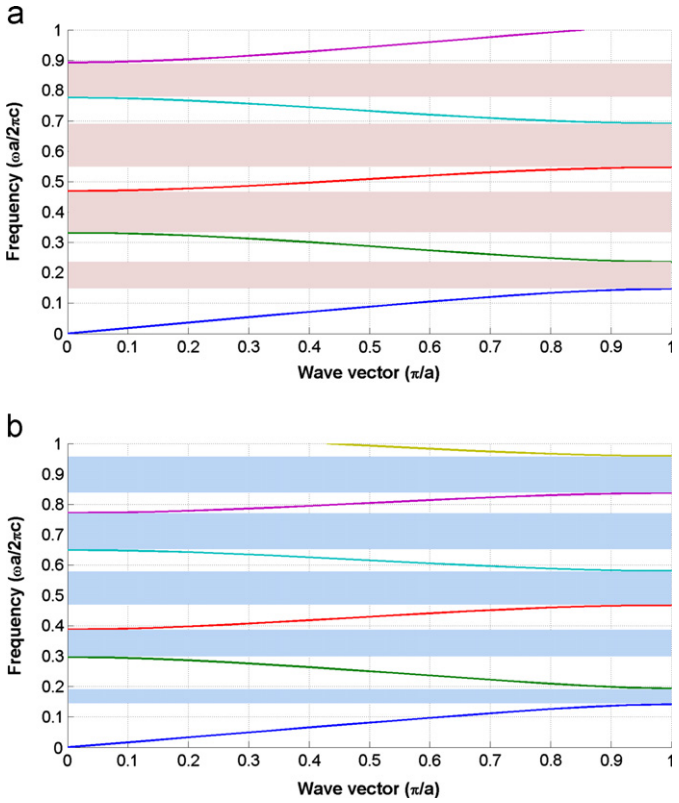

Fig. 4. Photonic band gap for (a) type 1 $(AB)_p$ at a filling factor $ff=0.55$ and (b) type 2 $(AC)_p$ at a filling factor $ff=0.69$.

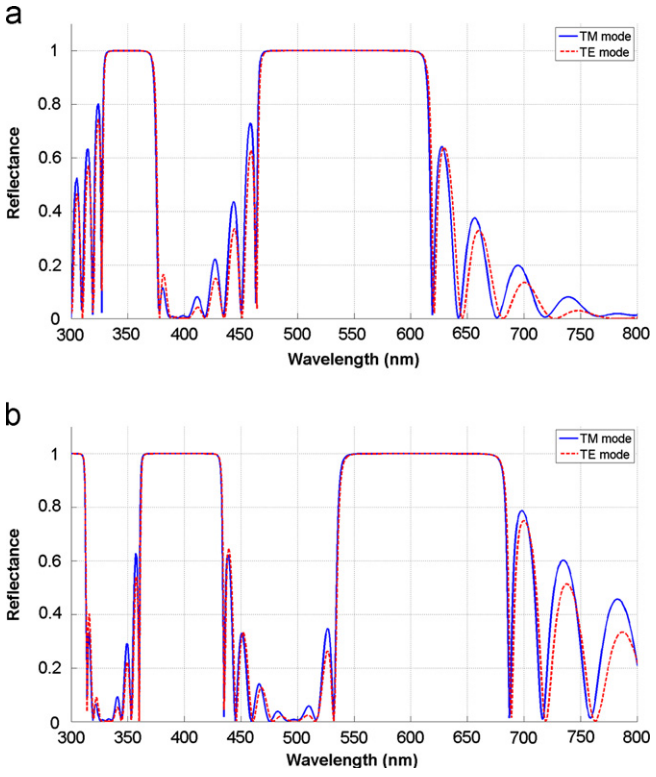

Fig. 5. Reflectance spectra of E (dashed line) and H-polarization (solid line) for (a) type 1 and (b) type 2 in the wavelength range 300 nm–1100 nm with the starting radius $\rho_0=80$ nm and the periodicity $p=8$.

molecular orientation of LC is disordered. At this state, the refractive index is $n_{LC}=\sqrt{(2n_o^2+n_e^2)/3}=1.56$, where the subscripts stand for ordinary and extraordinary, respectively. When the LC is homeotropic state, the molecular orientation of LC will parallel with the direction of applied electric field. Therefore, the refractive index of LC will change from n_{LC} to n'_{LC} and the refractive index can be consider as $n'_{LC}=n_o=1.49$, where the subscripts stand for ordinary [18,19]. In Fig. 7(a), the PBG was located at wavelength $\lambda=420$ nm to $\lambda=910$ nm and there are two pass-bands around $\lambda=575$ nm. When the electric field was applied, the pass-band at longer wavelength will disappear but something special happened to another pass-band. As indicated in Fig. 7(b), the reflectance of the pass-band at shorter wavelength decreases from 0.75 to 0.05 in the TM mode, but it's almost the same as in the TE mode. After that, we changed the azimuth mode from $m=0$ to $m=1$, the PBG was nearly invariant as $m=0$ shown in Fig. 8(a). When the external electric field is turned on, the reflectance of the defect mode remains unchanged in the TM mode but the reflectance was decrease substantially from 0.75 to 0.05 in the TE mode. The result of azimuth mode $m=1$ is contrary to azimuth mode $m=0$. If the starting radius is getting larger, the feature will disappear. Therefore, this phenomenon is caused by the effect of small starting radius.

4. Conclusion

In summary, we take advantage of the conception of PQW structure to broaden the PBG of cylindrical PCs. The PBG of our structure was demonstrated to be widened for azimuthal mode $m=0$ and $m=1$. Moreover, we created a defect mode by partially matching the PBG of type 1 and pass-band of type 2, then replaced air with LCs for tunability. According to the property of LCs, the phase of LCs under an applied electric field will change from pseudo-isotropic to

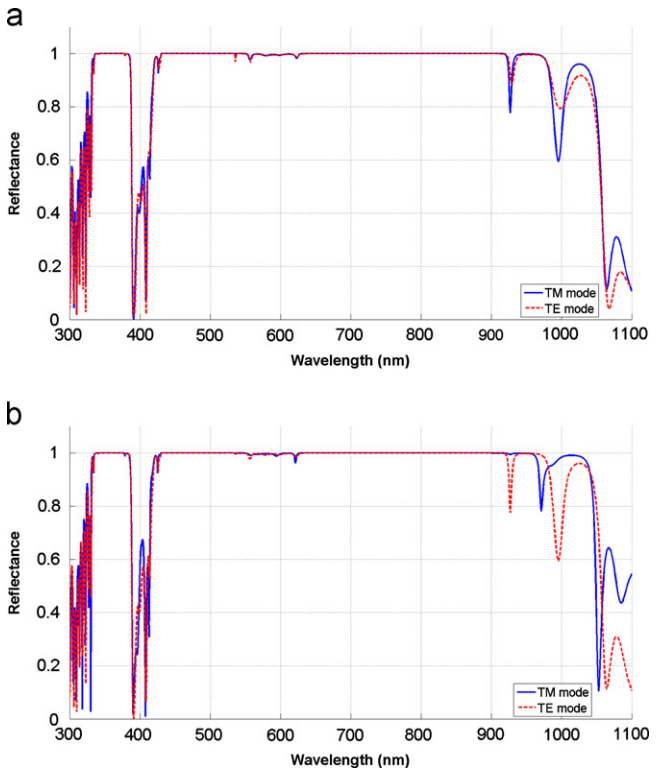

Fig. 6. Reflectance spectra of CPQW structure $(AB)_4(AC)_4(AB)_4$ in the TE (dashed line) and TM mode (solid line) for (a) azimuthal mode $m=0$ and (b) $m=1$.

homeotropic state and the refractive index will also change from $n_{LC}=1.56$ to $n'_{LC}=1.49$. From reflectance spectrum of CPQW structure with LCs, there are two narrow pass-bands around wavelength

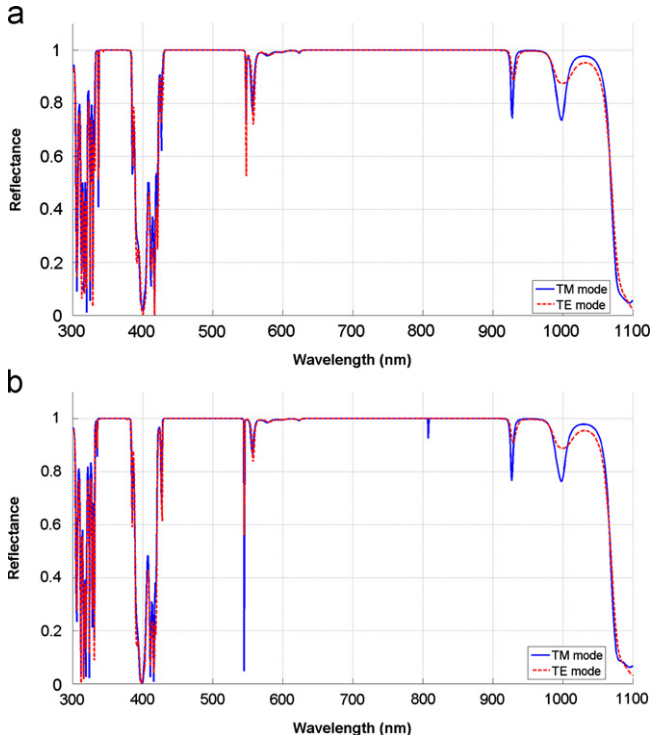

Fig. 7. Reflectance spectra of CPQW structure with LC defect layers in the TE (dashed line) and TM mode (solid line) at (a) pseudo-isotropic state and (b) homeotropic state, for azimuthal mode $m=0$. The reflectance of pass-band decrease from 0.75 to 0.05 in the TM mode and the reflectance were changeless in the TE mode.

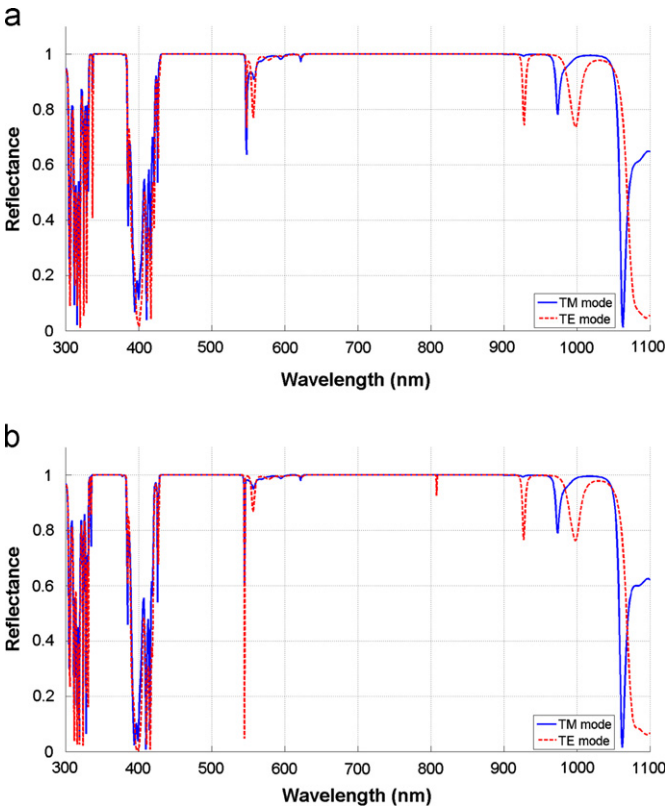

Fig. 8. Reflectance spectra of CPQW with LC defect layers in the TE (dashed line) and TM mode (solid line) at (a) pseudo-isotropic state and (b) homeotropic state, for azimuthal mode $m=1$. The reflectance is the same as in the TM mode, but the reflectance in the TE mode was decrease substantially to 0.05.

575 nm when the LCs are pseudo-isotropic and the azimuthal mode $m=0$. If the electric field is turned on, the reflectance of the shorter wavelength pass-band decreases from 0.75 to 0.05 in the TM mode but the reflectance in the TE mode is almost unchanged. For the mode order $m=1$ and the LCs are pseudo-isotropic state, the PBG and the defect mode remain the same as $m=0$. However, the result was reversed when the state of LCs are changed from pseudo-isotropic to homeotropic state. The reflectance of the defect mode in the TM mode is the same as the reflectance of pseudo-isotropic state, but the reflectance in the TE mode decreases substantially from 0.75 to 0.05. This novel feature will become insignificant when the starting radius ρ_0 is increased. The notable feature of the switchable tunneling mode may potentially be applied to communication components or optical devices such as sensor, filter and polarizer.

Acknowledgment

This work was supported by the National Science Council of the Republic of China, Taiwan, through the Grant nos. NSC-98–2112-M-009–019-MY2 and NSC-99–2112-M-216-002.

References

[1] E. Yablonovitch, Physical Review Letters 58 (1987) 2059.
[2] S. John, Physical Review Letters 58 (1987) 2486.
[3] E. Yablonovitch, T.J. Gmitter, Physical Review Letters 63 (1989) 1950.
[4] H. Benisty, D. Labilloy, C. Weisbuch, Applied Physics Letters 76 (2000) 532.
[5] M. Thiel, M. Hermatschweiler, M. Wegener, Applied Physics Letters 91 (2007) 123515.
[6] Z. Zhang, M. Dainese, L. Wosinski, S. Xiao, M. Qiu, Applied Physics Letters 90 (2007) 041108.
[7] P. Yeh, Optical Waves in Layered Media, John Wiley & Sons, Singapore, 1991.
[8] M.A. Kaliteevski, R.A. Abram, V.V. Nikolaev, Journal of Modern Optics 46 (1999) 875.
[9] C.J. Wu, S. Gwo, Journal of Electromagnetic Waves and Applications 21 (2007) 821.
[10] C. Xu, D. Han, X. Wang, X. Liu, J. Zi, Applied Physics Letters 90 (2007) 061112.
[11] C.S. Kee, J.E. Kim, H.J. Park, Physical Review B 61 (2000) 15523.
[12] B. Li, J. Zhou, L. Li, Applied Physics Letters 83 (2003) 4704.
[13] V.Y. Zyryanov, S.A. Myslivets, V.A. Gunyakov, Optics Express 18 (2010) 1283.
[14] D.J.J. Hu, P. Shum, C. Lu, X. Sun, G. Ren, X. Yu, G. Wang, Optics Communications 282 (2009) 2343.
[15] S. Bhuvneshwer, A. Bhargava, Progress in Electromagnetics Research Letters 27 (2011) 43.
[16] H.T. Hsu, M.H. Lee, T.J. Yang, Y.C. Wang, C.J. Wu, Progress in Electromagnetics Research Letters 117 (2011) 379.
[17] L.M. Zhao, B.Y. Gu, Y.S. Zhou, J.C. Wang, Modern Physics Letters B 18 (2004) 1293.
[18] I.C. Khoo, Journal of Modern Optics 37 (2007) 1801.
[19] V.A. Tolmachev, E.V. Astrova, Y.A. Pilyugina, T.S. Perova, R.A. Moore, J.K. Vij, Optical Materials 27 (2004) 831.